Characterization of ruthenium-dinitrogen tetraamine complexes by XAFS spectroscopy

Kaoru Okamoto,[a] Toshikazu Takahashi,[b] Kenji Kohdate,[a] Hiroshi Kondoh,[a] Toshihiko Yokoyama,[a] and Toshiaki Ohta[a]

[a]Department of Chemistry, School of Science, The University of Tokyo, 7-3-1 Hongo, Bunkyo-ku, Tokyo 113-0033 , Japan, [b]National Institute for Advanced Interdisciplinary Research, 1-1-4 Higashi, Tsukuba-shi, Ibaraki 305-8562, Japan. E-mail: ohta@chem.s.u-tokyo.ac.jp

A reaction between N_2 and *trans*-$Ru^{II}Cl_2L$ (L=2,5,9,12-tetramethyl-2,5,9,12-tetraazatridecane) in aqueous solutions has been investigated by XAFS spectroscopy. Ru *K*-edge EXAFS clearly revealed that there exists an N_2-bridged binuclear complex and that the Ru-Ru distance is 4.96 Å with the coordination number of 0.5. The Ru *K*-edge energies of the N_2 complexes are closer to that of $Ru^{III}Cl_2L^+$ rather than that of $Ru^{II}Cl_2L$, indicating back donation from the Ru dπ to the N_2 π* orbitals.

Keywords: dinitrogen bridging, binuclear ruthenium complex

1. Introduction

Since Harrison & Taube (1967) first prepared N_2-ruthenium complexes with an atmospheric N_2, molecular dinitrogen uptake and N-N bond cleavage by metal complexes have been extensively studied for the purpose of mimicking nitrogenase and developing nitrogen-fixing catalyses which will work under mild conditions. XAFS spectroscopy has shed light on materials which are unstable and cannot be isolated; Laplaza *et al.* (1996) clearly revealed by Mo-*K* EXAFS that $Mo[N(C(CD_3)_2CH_3)(3,5\text{-}C_6H_3(CH_3)_2)]_3$ reacts with N_2, generating an N_2-bridged binuclear complex which is stable only at low temperatures and decomposed to a nitrido complex when warmed to room temperature.

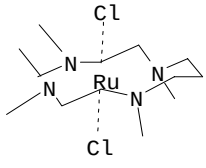

Takahashi *et al.* (1993, 1994) found that *trans*-$Ru^{II}Cl_2L$ (L=2,5,9,12-tetramethyl-2,5,9,12-tetraazatridecane, see inset) reacts with N_2 in aqueous solutions and produces NO under oxidizing conditions. Under 1 atm of N_2, a 1:1 substitution occurs and $RuClLN_2^+$ salt is isolated, but under 0.1 atm of N_2, there exists other species. Although it is inferred to be a dinitrogen-bridged binuclear complex from NMR and Raman spectroscopies, this species exists only in HCl solutions and no direct evidence has been obtained. The purpose of this study is to identify the local structures of the reaction intermediates directly by XAFS spectroscopy.

2. Experimental

The preparation method of the starting complex, $[Ru^{III}Cl_2L]Cl$, has been reported elsewhere (Takahashi *et al.*, 1993). 1 mol dm^{-3} HCl solutions of this Ru^{III} complex (ca. 0.2 mol dm^{-3}) were reduced to Ru^{II} with excess $TiCl_3$ (1 mol dm^{-3} HCl solution) and then allowed to stand for several days under N_2 (sample A) or $N_2$10%-Ar90% (sample B). The aqueous solutions of $Ru^{III}Cl_2L^+$, $Ru^{II}Cl_2L$, and sample A were diluted with ethanol, then evacuated and sealed in glass cells for low-temperature (ca. 210 K) measurements. On the other hand, since sample B is decomposed with ethanol dilution, its aqueous solution was sealed in a polyethylene bag (0.08 mm thickness) with a fluorocarbon spacer under $N_2$10%-Ar90% gas, and measured at room temperature. Taube's complex $[Ru(NH_3)_5]_2(\mu\text{-}N_2)Cl_4$ was prepared with the method by Allen et al. (1970) and measured as a reference material at about 30 K.

All measurements were carried out at Photon Factory (operation energy of 2.5 GeV and stored current of 400–200 mA). Ru *K*-edge XAFS spectra were collected in the transmission mode at the Beamline 10B using a Si(311) monochromator. The intensities of the incident (I_0) and transmitted (I) x-rays were recorded using ionization chambers filled with Ar50%-$N_2$50% and Ar50%-$N_2$50% or Ar100%, respectively. The relative energy was calibrated with two glitches appearing near the Ru-*K* edge in the I_0 function, and the error was estimated to be about 0.5 eV from the interval between the glitches. The integration time was 16 s/point except for sample B, for which it was 36 s/point to obtain higher statistics.

3. Results and discussion

Figure 1 shows Ru *K*-edge XANES spectra of the four complexes. Each of these exhibits a broad edge with two major post-edge components, though one at about 22130 eV is slightly enhanced after N_2 treatment (*i.e.* for samples A and B). The edge shows a shift to a lower energy when reduced from Ru^{III} to Ru^{II}, which shifts back to a higher energy after N_2 treatment. This is probably due to an increase of the positive charge on Ru in N_2 complexes caused by back donation from Ru d_π to N_2 π* orbitals.

Figure 2 shows the Ru *K*-edge EXAFS functions $k^3\chi(k)$ and their Fourier transforms (FT). For sample B, one can see a component with a short period at k>12 $Å^{-1}$ in $k^3\chi(k)$ (Fig. 2d, left) and a peak at about 4.6 Å in the Fourier transforms (Fig. 2d, right), which also appear in those of $[Ru(NH_3)_5]_2(\mu\text{-}N_2)^{4+}$ powder (Fig. 2e) but not in those of the other samples. Although the peak of sample B is weak when the k range in Fourier transform is as narrow as 2.65–11.75 $Å^{-1}$ (Fig. 2d, dashed line), it gains intensity when its upper limit is larger than 14.0 $Å^{-1}$ (Fig. 2d, solid and dot-dashed lines), while no peak appears for other tetraamine samples with the same k range. This is the reason why the data for sample B were taken up to k~18 $Å^{-1}$ with a longer integration time. This 4.6 Å peak can be attributed to the Ru-Ru shell as that of $[Ru(NH_3)_5]_2(\mu\text{-}N_2)^{4+}$, and it clearly indicates the existence of

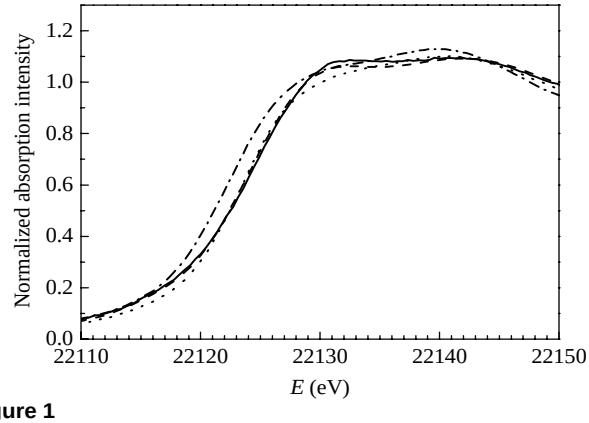

Figure 1
XANES spectra for $Ru^{III}Cl_2L$ (dotted line), $Ru^{II}Cl_2L$ (dot-dashed line), sample A (solid line), and sample B (dashed line).

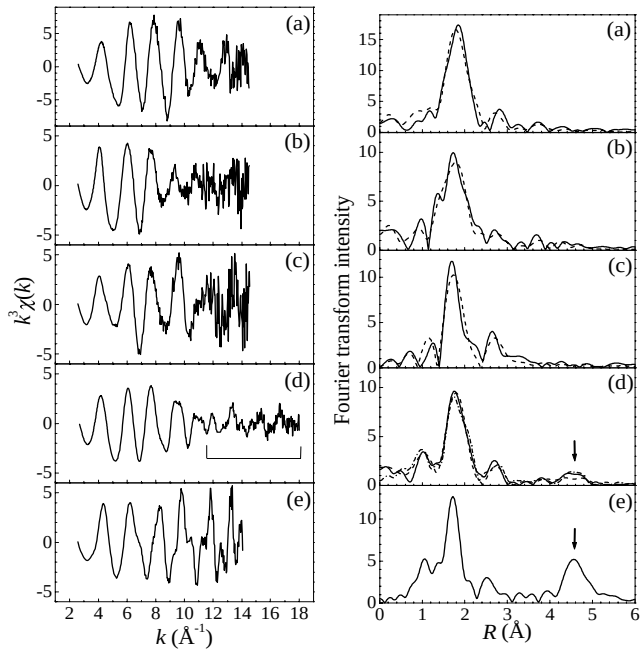

Figure 2
EXAFS functions $k^3\chi(k)$ (left) and Fourier transforms (right) for $Ru^{III}Cl_2L^+$ (a), $Ru^{II}Cl_2L$ (b), sample A (c), sample B (d), and $[Ru(NH_3)_5]_2(\mu\text{-}N_2)^{4+}$ (e). The FT k ranges are 2.6~12 Å^{-1} (dashed lines), 2.6~14 Å^{-1} (solid lines), and 2.6~15.5 Å^{-1} (dot-dashed lines).

an N_2-bridged binuclear complex. The k-dependence of the peak intensity could also be explained by this assignment, as shown later in Fig. 3. The peak of sample B is much weaker than that of $[Ru(NH_3)_5]_2(\mu\text{-}N_2)^{4+}$. This is because sample B is a mixed solution of binuclear and mononuclear complexes and was measured in room temperature, while powdery $[Ru(NH_3)_5]_2(\mu\text{-}N_2)^{4+}$ was measured at low temperature.

There are two possible N_2-bridging configurations: end-on and side-on. In an end-on configuration, the M-N-N-M chain is almost linear and the M-M shell will be enhanced due to the multiple-scattering focusing effect (Stern, 1988). However, in a side-on configuration, where the M-M and the N-N axes are perpendicular to each other, the M-M shell with a long distance would be very weak in solutions at room temperature. This suggests that Ru-N_2-Ru in sample B should have an end-on configuration. This is consistent with the fact that the M-M distances are generally ~5 Å in end-on complexes while they are 3–4 Å in side-on ones. One of the possible structures is shown in the inset. The other peaks at 1–3 Å can be attributed to the Ru-N(L), Ru-Cl, Ru-C(L), and two Ru-N(N_2) (for samples A and B).

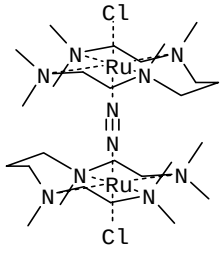

In order to obtain the interatomic distance of each shell, the curve fitting analyses were performed with the analysis code EXAFSH (Yokoyama *et al.*, 1993). The data were Fourier-filtered before fitting and the k and R ranges are tabulated in Table 1. The theoretical EXAFS amplitude and phase-shift functions were calculated using FEFF8 (Ankudinov *et al.*, 1998) for an octahedral *trans*-$RuCl_2(N(CH_3)_3)_4$ and its N_2-substituted mononuclear and binuclear complexes. The interatomic distances in these model complexes referred to known crystal structures of

Table 1
k- and R-ranges used in the analysis.

	Δk_{FT} (Å^{-1})	ΔR_{fit}(Å)	Δk_{fit} (Å^{-1})
$Ru^{III}Cl_2L$	2.7–11.5	1.0–3.1	3.2–11.0
$Ru^{II}Cl_2L$	2.6–11.1	1.15–3.15	3.1–10.6
Sample A	2.65–10.65	0.95–3.25	3.15–10.15
Sample B (1–3 Å shells)	2.65–11.75	0.9–3.1	3.15–11.25
(4.6 Å shell)	3.7–15.5	4.15–4.9	4.2–15.0
$[Ru(NH_3)_5]_2(\mu\text{-}N_2)$	3.9–13.8	4.1–5.1	4.4–13.3

trans-$[Ru^{III}Cl_2L]Cl$ and $[Ru(NH_3)_5]_2(\mu\text{-}N_2)Cl_4$. For the 1–3 Å shells, the coordination numbers N and the edge-energy shifts ΔE_0 were fixed, while the distances R and the Debye-Waller factors C_2 were optimized except C_2(Ru-C)'s of samples A and B and C_2(Ru-N-N) for sample B. For the 4.6 Å shell, N, R, and C_2 were optimized. The intrinsic factor S_0^2 for the Ru-Ru shell was set to the value obtained for $[Ru(NH_3)_5]_2(\mu\text{-}N_2)Cl_4$ (0.71), and those for the others were to 1.0. Higher-order cumulants of the Debye-Waller factor were neglected.

A multishell fitting is required for the 1–3 Å shells. Firstly, curve fitting for a $Ru^{III}Cl_2L^+$ solution was performed and then the results are compared with those of single crystal x-ray diffraction. The tetraamine L has thirteen carbon atoms at different distances: six methylene and six methyl bound to the nitrogen, and one between two carbon atoms. Because the independent data points are limited to $2\Delta k_{fit}\Delta R_{fit}/\pi$ +1=10–12, thirteen Ru-C shells should be convoluted. Two-shell fitting worked well while only one Ru-C shell fitting did not. The results were not affected by the total number of carbon atoms, twelve or thirteen, and the coordination numbers, n and 12–n or 13–n with n from four to eight. Thus, the carbon atoms were grouped into methylene and methyl atoms with the coordination number of six for each, and the farthest one was ignored. The fitting results tabulated in Table 2 show a good agreement with the averaged crystal structure within the errors although the Ru-Cl distance is slightly longer in the EXAFS results. Analyses for the other complexes were carried out in a similar manner and the results were also tabulated in Table 2. While sample A is known to have a structure of $RuClLN_2^+$, sample B is probably a mixture of $RuClLN_2^+$and $[RuClL]_2(\mu\text{-}N_2)^{2+}$, as indicated from UV-vis spectroscopy. However, because the difference is expected to be small except for being binuclear, it was analyzed as $[RuClL]_2(\mu\text{-}N_2)^{2+}$ and the results would be the average of these two complexes. Though a wider energy-range data were obtained for sample B, the k ranges for the 1–3 Å shells were set as narrow as for the other samples to compare the fitting results. The 4.6 Å peak is successfully fitted with a Ru-Ru shell including multiple scattering along Ru-N-N-Ru, and the results are tabulated in Table 3 together with the Fourier-filtered EXAFS functions in Fig. 3.

The coordination number and the distance of Ru-Ru are 0.5 and 4.96 Å, respectively. The ratio of the binuclear complex at this concentration was estimated at 40–80% by UV-vis and NMR spectroscopies, and it was now confirmed directly by EXAFS spectroscopy. The distance is nearly the same with other Ru-N_2 binuclear complexes.

Analysis on the 1–3 Å peaks was very complicated due to the contributions from many shells and precise discussion would be almost impossible, however, it provides some insights on the structures. The Ru-N(N_2) distance in $RuClLN_2^+$ and $[RuClL]_2(\mu\text{-}N_2)^{2+}$ is 1.93 and 1.89 Å, respectively, which are much shorter

Table 2

The curve fitting results for the 1–3 Å shells, together with the single crystal x-ray diffraction results on $Ru^{III}Cl_2L^+$. Values in square brackets are fixed and those in parentheses are errors on the last significant digit.

	$Ru^{III}Cl_2L^+$				$Ru^{II}Cl_2L$			Sample A			Sample B		
	N	XRD *R* (Å)	*R* (Å)	C_2(10^{-2}Å^2)	*N*	*R* (Å)	C_2(10^{-2}Å^2)	*N*	*R* (Å)	C_2(10^{-2}Å^2)	*N*	*R* (Å)	C_2(10^{-2}Å^2)
Ru-N(L)	[4]	*2.186*	2.17(1)	0.6(1)	[4]	2.19(1)	0.6(2)	[4]	2.20(2)	0.4(3)	[4]	2.15(3)	0.5(5)
Ru-Cl	[2]	*2.337*	2.353(5)	0.16(5)	[2]	2.45(1)	0.9(2)	[1]	2.38(2)	0.3(3)	[1]	2.43(2)	0.1(2)
Ru-C(methylene)	[6]	*2.966*	3.00(4)	1.3(6)	[6]	3.08(3)	1.0(4)	[6]	2.98(7)	[1.0]	[6]	2.99(9)	[1.0]
Ru-C(methyl)	[6]	*3.149*	3.20(2)	0.5(3)	[6]	3.26(3)	0.8(4)	[6]	3.17(7)	[1.0]	[6]	3.15(9)	[1.0]
Ru-N-N	-	-	-	-	-	-	-	[1]	1.93(5)	0.3(7)	[1]	1.89(5)	0.2(8)
Ru-N-N	-	-	-	-	-	-	-	[1]	3.03(3)	0.2(4)	[1]	3.05(5)	[0.2]
ΔE_0 (eV)			[-8.5]			[-8.5]			[-8.5]			[-8.5]	
R-factor[§](%)			3.44			10.7			2.86			13.8	

[§]R-factor is defined as $R = \sqrt{\sum_i \left\{k_i^n \chi_{\text{obs}}(k_i) - k_i^n \chi_{\text{calc}}(k_i)\right\}^2 \Big/ \sum_i \left\{k_i^n \chi_{\text{obs}}(k_i)\right\}^2}$.

Table 3

The curve fitting results for the 4.6 Å shells.

	$[Ru(NH_3)_5]_2(\mu\text{-}N_2)$			Sample B		
	N	*R* (Å)	C_2(10^{-2}Å^2)	*N*	*R* (Å)	C_2(10^{-2}Å^2)
Ru-Ru	[1]	4.981(6)	0.28(6)	0.5(2)	4.96(2)	0.5(1)
ΔE_0 (eV)		[-3.0]			[-3.0]	
R-factor[§](%)		5.14			5.49	

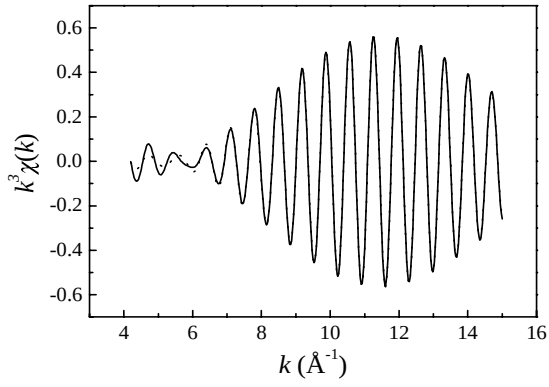

Figure 3

The Fourier-filtered EXAFS functions for the Ru-Ru shell; experimental data (solid line) and theoretical calculations (dotted line).

than those of Ru-N(L), suggesting a strong interaction between Ru and N_2. Moreover, the N-N distances obtained from the differences of Ru-N-N and the Ru-N-N distances were 1.10 and 1.16 Å, respectively. Longer N-N distances than that of N_2 molecule (1.098 Å) are expected also from IR and Raman spectroscopy; the ν(NN) for sample A and B were ca. 2070 and 2029 cm^{-1}, respectively, being much smaller than that of N_2 molecule, 2358 cm^{-1}. However, further discussion about the N-N distances is difficult due to relatively large analysis errors in the fitting procedure.

A distinct shortening of the Ru-Cl distance in $RuClLN_2^+$ is found in Table 3. This could be due to the reduced d_π electron density on Ru caused by π-back donation from Ru to N_2 as we suggested from the XANES spectra. On the other hand, the Ru-Cl bond is elongated for $[RuClL]_2(\mu\text{-}N_2)^{2+}$, which might be explained by the influence of the repulsion between the methyl groups in tetraamine.

Thus, the structure of a binuclear complex with linear Ru-N-N-Ru has successfully been determined with some information about electronic state on the metal and the N_2 molecule. To confirm these results, we are planning to perform Ru *L*-edge XANES measurements in solutions.

The present work has been performed under the approval of Photon Factory Program Advisory Committee (PF-PAC No. 99G286).

References

Allen, A. D., Bottomley, F., Harris, R. O., Reinsalu, V. P. & Senoff, C. V. (1970). *Inorg. Synth*. **12**, 2-9.

Ankudinov, A. L., Ravel, B., Rehr, J. J. & Conradson, S. D. (1998). *Phys. Rev.* **B58**, 7565-7576.

Harrison, D. E. & Taube, H. (1967). *J. Am. Chem. Soc.* **89**, 5706-5707.

Laplaza, C. E., Johnson, M. J. A., Peters, J. C., Odom, A. L., Kim, E., Cummins, C. C., George, G. N. & Pickering, I. J. (1996). *J. Am. Chem. Soc.* **118**, 8623-8638.

Stern, E. A. (1988). *X-ray Absorption: Principles, Applications, Techniques of EXAFS, SEXAFS and XANES, Chemical Analysis* vol. 92, edited by Koningsberger, D. C. & Prins, R., pp. 34-36. John Wiley & Sons Inc.

Takahashi, T., Hiratani, K. & Kimura E. (1993). *Chem. Lett.* **1993**, 1329-1332.

Takahashi, T. (1994). PhD thesis, Hiroshima University, Japan.

Yokoyama, T., Hamamatsu, H. & Ohta, T. (1993). EXAFSH version 2.1, The University of Tokyo.

Received 31 July 2000 • Accepted 30 October 2000